# Wounding of Bioengineered Skin: Cellular and Molecular Aspects After Injury

Vincent Falanga,*† Cary Isaacs,‡ Dana Paquette,* Gregory Downing,‡ Nicola Kouttab,§ Janet Butmarc,* Evangelos Badiavas,*§ and Jan Hardin-Young‡

*Departments of Dermatology and §Pathology, Boston University School of Medicine, Roger Williams Medical Center; †Boston University Department of Biochemistry, Boston, Massachusetts, U.S.A.; ‡Organogenesis Inc., Canton, Massachusetts, U.S.A.

**Skin substitutes are increasingly being used in the treatment of difficult to heal wounds but their mechanisms of action are largely unknown. In this study, using histology, immunostaining, flow cytometry, enzyme-linked immunosorbent assay, and reverse transcription polymerase chain reaction, we determined the response to injury of a human bilayered skin substitute. Meshing or scalpel fenestration of the construct was found to stimulate keratinocyte migration and to decrease proliferation. By 24 h, flow cytometry of the keratinocyte component showed that meshing was associated with a 33% decrease in the number of cells in S phase ($p < 0.01$). An approximately 2-fold decrease in staining for Ki67, a proliferation marker, was observed with meshing of human bilayered skin substitute. The process of reepithelialization was apparent by 12 h, however, the wounded human bilayered skin substitute was healed by day 3, and a stratum corneum and fully stratified epithelium were re-established by day 4. Reverse transcription polymerase chain reaction analysis and enzyme-linked immunosorbent assays showed that the expression of acute proinflammatory cytokines (interleukins 1α, 6, and 8, tumor necrosis factor α) peaked by 12–24 h postinjury. The levels of mRNA of certain growth factors (transforming growth factor β1, vascular endothelial growth factor, insulin-like growth factor 2) but not others (platelet-derived growth factors A and B, keratinocyte growth factor, fibroblast growth factors 1 and 7, transforming growth factor β3) increased by 12 h and peaked by 1–3 d after injury, returning to normal by day 6. Immunostaining for tumor necrosis factor α and transforming growth factor β1 paralleled these findings by reverse transcription polymerase chain reaction. We conclude that human bilayered skin substitute, as a prototypic bilayered skin substitute, is a truly dynamic living tissue, capable of responding to physical injury in a staged and specific pattern of cell migration, reepithelialization, and cytokine expression.** ***Key words: wound healing/tissue repair/skin substitute/keratocytes/cytokines/growth factors. J Invest Dermatol 119:653–660, 2002***

Over the last several years, advances in tissue culture and in the understanding of matrix proteins have made it possible for investigators to construct increasingly sophisticated skin substitutes. Some of the skin substitutes are acellular, some contain living cells, and others are bilayered, composed of both epidermal and dermal cell types. The cells used in the preparation of these bioengineered skin constructs are generally derived from neonatal foreskin, whereas the initial matrix scaffold in which the cells are grown varies from glycosaminoglycans, to bovine collagen, to synthetic materials (Phillips, 1998; Falanga, 2000*a*). There has been a great deal of interest in using these bioengineered skin constructs in the treatment of burns and chronic wounds, where the need to accelerate healing seems to be greatest. For at least two decades, investigators have used human keratinocyte sheets, either autologous or allogeneic, to treat burns and a variety of chronic wounds. More recently, the field has seen the approval by regulatory agencies of a bilayered skin substitute for the treatment of venous (Falanga *et al*, 1998; Brem *et al*, 2001) and diabetic foot ulcers (Veves *et al*, 2001).

There is increasing recognition that skin substitutes will have an important therapeutic role in ulcers that are difficult to heal and in those where acceleration of healing can prevent further complications. The mechanisms of action of bioengineered skin in wound repair is unclear, however. It has been argued that the cells in living skin substitutes act ''smart'' in engineering terms. This concept suggests that cells are able to sense and to adapt to their environment, and to act appropriately in terms of their synthetic repertoire, the dose and sequence of mediators produced, and the timing of release of cytokines and growth factors (Falanga *et al*, 1998; Phillips, 1998; Falanga, 2000*b*). This concept also suggests that skin substitutes may employ different mechanisms of action for acute and chronic wounds. There is at present only limited evidence for the mechanisms of action of bioengineered skin. In chronic wounds, the data to date indicate that cells from allogeneic skin substitutes are likely to have a very short life span in wounds, suggesting that the beneficial clinical effects of these living constructs are not due to a permanent replacement of cells (Brain

Manuscript received August 7, 2001; revised April 7, 2002; accepted for publication May 3, 2002.

Reprint requests to: Vincent Falanga, Professor of Dermatology and Biochemistry at Boston University, Department of Dermatology, Roger Williams Medical Center, 50 Maude Street, Providence, RI 02908. Email: vfalanga@bu.edu

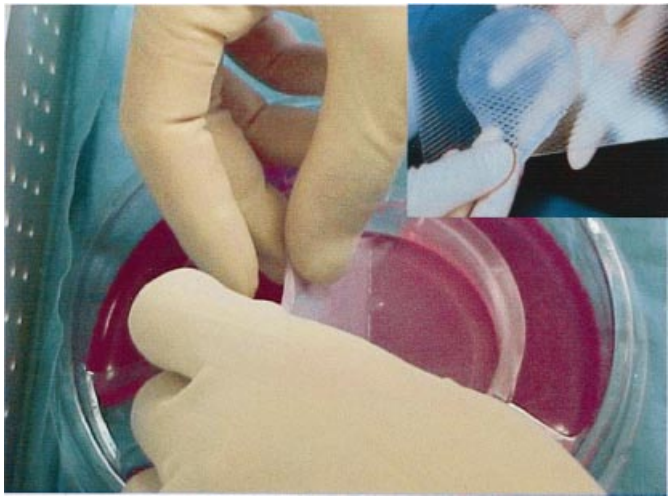

**Figure 1. Photomicrographs showing the HBSS as it is being lifted from its nutrient agar, and after meshing (inset).**

*et al*, 1989; Phillips *et al*, in press). Interestingly, investigators have found that the application of skin substitutes to previously nonhealing ulcers stimulates the edges of the wound to migrate toward the center, the ''edge effect''. This observation has been made with keratinocyte sheets as well as other types of bioengineered skin and it suggests that a major role of skin substitutes is to stimulate the endogenous healing process (Falanga, 2000*b*).

We have been interested in the mechanisms of action of bioengineered skin as a whole, and particularly in how constructs containing living cells are capable of stimulating the endogenous process of wound repair. We have first focused our attention on how skin substitutes behave in response to injury, and whether they are indeed capable of releasing cytokines and growth factors and going through a process of repair. An added advantage of this approach is that it can lead to fundamental insights into the healing process in a well-defined but complex *in vitro* environment, more similar to the *in vivo* situation. Also, many of the skin substitutes are meshed or manipulated before application to wounds, and therefore do go through a process of injury and repair. Therefore, it becomes vitally important and clinically relevant, even in terms of future improvements in these constructs, to know the events associated with injury to bioengineered skin.

## MATERIALS AND METHODS

**Human bilayered skin substitute (HBSS)** For these studies we used a prototypic construct, an HBSS, which is commercially available as Apligraf (Organogenesis, Canton, MA; licensed by Novartis Pharmaceuticals, East Hanover, NJ) and whose composition and construction have been previously described (Wilkins *et al*, 1994). HBSS contains human dermal fibroblasts in a contracted collagen lattice overlaid with a cornified epidermis. Keratinocytes and fibroblasts used in the preparation of HBSS are grown from infant foreskins according to published procedures (Wilkins *et al*, 1994; Falanga *et al*, 1998). Briefly, fibroblasts in suspension are mixed with a bovine type I collagen solution and poured into culture transwells (Costar, Cambridge, MA). The cultures are incubated for 6 d at 36°C, 10% $CO_2$. During that time the fibroblasts contract the collagen to form a cellular dermal matrix. Human keratinocytes are then seeded onto the surface of the lattice and the construct is submerged for 4 d in medium that allows the keratinocytes to cover the dermal matrix. After 4 d the constructs are cultured at the air–liquid interface to promote the development of the epidermis, which reaches maturity after 10 d at the air interface (Wilkins *et al*, 1994). In these studies HBSS was used at 10–11 d post-airlift. HBSS is easy to handle and to mesh, and therefore suitable for the types of experiments described in this report (**Fig 1**).

**Table I. Primer sequences used in RT-PCR for determining the expression of cytokines and growth factors after injury to bioengineered skin**

| Primers | Primer sequence |
|---|---|
| FGF-1 (5′) | gct gct gag gcc atg gct gaa |
| FGF-1 (3′) | aca gat ctc ttt aat cag aag aga ctg |
| FGF-2 (5′) | gga gtg tgt gct aac cgt tac ctg gct atg |
| FGF-2 (3′) | tca gct ctt agc aga cat tgg aag aaa aag |
| FGF-7 (5′) | ctt tgc tct aca gat cat gct ttc |
| FGF-7 (3′) | ttg cca tag gaa gaa agt ggg ctg |
| IL-1α (3′) | tag tgc cgt gag ttt ccc aga aga aga gga gg |
| IL-1α (5′) | caa gga gag cat ggt ggt agt agc aac caa cg |
| IL-6 (3′) | gaa gag ccc tca ggc tgg act g |
| IL-6 (5′) | atg aac tcc ttc tcc aca agc gc |
| IL-8 (3′) | tct cag ccc tct tca aaa act tct c |
| IL-8 (5′) | atg act tcc aag ctg gcc gtg gct |
| PDGF-A (3′) | ctg ctt cac cga gtg cta caa tac ttg ct |
| PDGF-A (5′) | aga agt cca ggt gag gtt aga gga gca t |
| PDGF-B (3′) | gcc gtc ttg tca tgc gtg tgc ttg aat ttc cg |
| PDGF-B (5′) | ctg tcc agg tga gaa aga tcg aga ttg tgc gg |
| TGF-α (3′) | ggc ctg ctt ctt ctg gct ggc a |
| TGF-α (5′) | atg gtc ccc tcg gct gga cag |
| TGF-β1 (3′) | agg ctc caa atg tag ggg cag g |
| TGF-β1 (5′) | gcc ctg gac acc aac tat tgc t |
| TGF-β3 (5′) | att acc tcc aag gtt ttc cg |
| TGF-β3 (3′) | gcc cgc ttc ttc ctc tga cc |
| TNF-α (3′) | gca atg atc cca aag tag acc tgc cca gac t |
| TNF-α (5′) | gag tga caa gcc tgt agc cca tgt tgt agc a |
| GAPDH (3′) | cat gtg ggc cat gag gtc cac cac |
| GAPDH (5′) | tga agg tcg gag tca acg gat ttg gt |

***In vitro* wounding** HBSS was wounded by passing it through a skin mesher (1.5 cm × 1 cm, Zimmer, Dover, OH), so as to create a 1.5–1 meshing ratio. For cytokine studies and for histologic evidence of reepithelialization, cultures were kept at the air–liquid interphase and incubated at 37°C. Biopsies of the HBSS and culture supernatants were collected at 4 and 12 h, and at 1, 2, 3, and 6 d after wounding. Two biopsies were taken at each time point. One biopsy was used for RNA isolation for reverse transcription polymerase chain reaction (RT-PCR) analysis and another biopsy was used for hematoxylin and eosin staining for routine histologic analysis. The supernatant was removed for enzyme-linked immunosorbent assay (ELISA) analysis. In other experiments, the HBSS was injured by multiple 0.4 cm excisions, approximately 1.5 cm apart, using a scalpel with a #15 blade (fenestration). The injured HBSS was fully expanded and placed on its dermal component (i.e., the same construct but without epidermis). In other experiments, HBSS was either kept or placed back in its transwell, over the nutrient agar, immediately after injury by meshing or fenestration. In that case, the construct was either left undisturbed (control unlifted), lifted from its agar nutrient transwell (control lifted), fenestrated with a scalpel, or meshed at a ratio of 1.5–1. The culture medium used during and after injury to HBSS consisted of the following formulation: Dulbecco's modified Eagle's medium 48%, Ham's nutrient mixture F-12 48%, L-glutamine 658 mg per liter, hydrocortisone 0.4 mg per liter, insulin 5.0 mg per liter, human transferrin 5.0 mg per ml, triiodothyronine 13.5 ng per liter, ethanolamine 0.1 mM, O-phosphoethanolamine 14.0 mg per liter, selenious acid 6.78 μg per liter, adenine 24.4 mg per liter, newborn bovine serum 1.0%.

We also performed studies for determining the cytokine profile of the dermal equivalent of HBSS. In this case, the dermal equivalent (without keratinocyte component) was minced with a scalpel and its cytokine profile at 7, 14, and 21 d was determined by RT-PCR.

**Histologic processing** Samples of HBSS were fixed in 10% neutral buffered formalin, rinsed in phosphate-buffered saline (PBS), dehydrated through graded ethanols, cleared, infiltrated, and embedded in paraffin. Five micron sections were cut on a microtome, affixed to glass microscope slides, dried, and then deparaffinized and hydrated.

**Immunohistochemistry** Immunohistochemistry was performed on formalin-fixed tissue. Briefly, the tissue was first deparaffinized and treated with methanol hydrogen peroxide. Antigen retrieval was

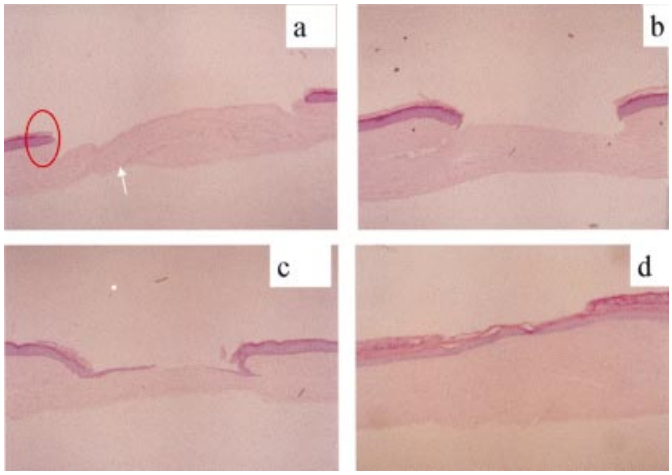


**Figure 2. Photomicrographs showing the process of reepithelialization of the HBSS after injury and application to its dermal equivalent.** (*a*) After injury. A circle has been placed over the cross-section of HBSS, and the arrow indicates the dermal equivalent. 20×. (*b*) Appearance of construct 12 h after injury. 20×. (*c*) Appearance of healing construct at day 2. 20 ×. (*d*) Healed construct at day 4. 20×.

performed with 0.01 M citric acid pH 6.0 using a steamer for 20 min. Slides were placed in 1 × PBS with blocking serum (horse serum for monoclonals and goat serum for the rabbit polyclonal antibodies). The tissue was then treated with the primary antibody for 1 h at room temperature. For these experiments, the primary antibodies were diluted with 1 × PBS and 0.1% bovine serum albumin. Secondary antibodies were incubated with the sections for 1 h at room temperature. Secondary antibodies were either antimouse horse IgG (dilution 1:200 for mouse primary antibodies) or antirabbit goat IgG (dilution 1:200 for rabbit primary antibodies). Both antibodies were from Vector (Burlingame, CA). The tertiary antibody was streptavidin horseradish peroxidase conjugated (DAKO, Carpinteria, CA) diluted 1:400 and incubated with the sections for 1 h at room temperature. Following that step, the sections were treated with 3,3-diaminobenzidine tetrahydrochloride (Zymed, San Francisco, CA) for 10 min and 0.5% cupric sulfate in 0.9% NaCl for 5 min. The sections were counterstained with hematoxylin (DAKO) for 10 s. We used the following primary antibodies: antihuman rabbit transforming growth factor β1 (TGF-β1) (V) (Santa Cruz Biotech, Santa Cruz, CA), at a dilution of 1:70; antihuman mouse tumor necrosis factor α (TNF-α) (1E8-G6, Santa Cruz), at a dilution of 1:30; antihuman mouse Ki67 at a dilution of 1:50 (Beckman Coulter, Miami, Fl, and DAKO).

**Flow cytometry** Flow cytometry of the keratinocyte component of HBSS was performed 24 h after scalpel or meshing injury, in the experiments where the construct was placed back on its nutrient agar. The processing of HBSS for cell cycle analysis was performed according to the following procedures. A section of HBSS (3 × 3 cm) was removed from its transwell, placed in 15 ml of thermolysin (0.5 mg per ml; Sigma, St. Louis, MI), and incubated at 37°C for 2 h. The tissue was then moved to a tissue culture dish containing 10 ml of PBS. The epidermis was separated from the dermis by gentle teasing with forceps. In preparing the keratinocyte suspensions, the cells were disaggregated in PBS utilizing a Medi machine (BD, St. Jose, CA) and a 50 μm filcon filter (BD), and cell viability (> 95%) was verified using trypan blue exclusion. Subsequently, the cells were washed in PBS and resuspended in propidium iodide solution (DNA-Assay, New Concept Scientific, Niagra Falls, NY), at a concentration of $1 \times 10^6$ cells per ml. Entry into the S phase of the cell cycle and proliferative activity of cells derived from dermis and epidermis was determined from a FACS Caliber flow cytometer (Becton Dickinson, St. Jose, CA). Cells were acquired using CELLQuest software program (BD) with doublet discrimination. At least 25,000 events were acquired for each sample. The cells were then analyzed utilizing the ModFIT LT software program (Verity Software House, Topsham, ME).

**Cytokine detection by RT-PCR and ELISA** HBSS samples were extracted using the Qiagen (Valencia, CA) Shredder/RNeasy extraction procedure on approximately 0.5 $cm^2$ biopsy. Moloney murine leukemia virus (MMLV) reverse transcriptase was used to synthesize complementary strands of DNA (cDNA). The PCR actual primers used are shown in **Table I**. For each primer, the following concentrations and reaction mix were used: 5 μl cDNA from the above procedure was added to 31 μl DEPC-treated water, 5 μl 10 × PCR buffer, 1 μl 10 mM dATP, 1 μl 10 mM dTTP, 1 μl 10 mM dGTP, 1 μl 10 mM dCTP, 3 μl 25 mM $MgCl_2$, and 0.4 μl Amplitaq enzyme in thin-walled reaction tubes. A 2% agarose gel containing 1 ng per ml ethidium bromide was viewed under ultraviolet light (312 nm). Stained gels were photographed, and subsequently digitally captured using a CCD camera. Intensities of band products were quantified using image analysis software (ImagePro, CA). Each of the cytokine measurements was corrected for varying amounts of RNA by normalizing to glyceraldehyde-3-phosphate dehydrogenase (GAPDH). Supernatants were also collected and frozen at 60°C until ready to be tested. Interleukin-1α (IL-1α) and IL-6 protein levels were measured using R&D ELISA kits (R&D Systems, Minneapolis, MN) according to the manufacturer's instruction.

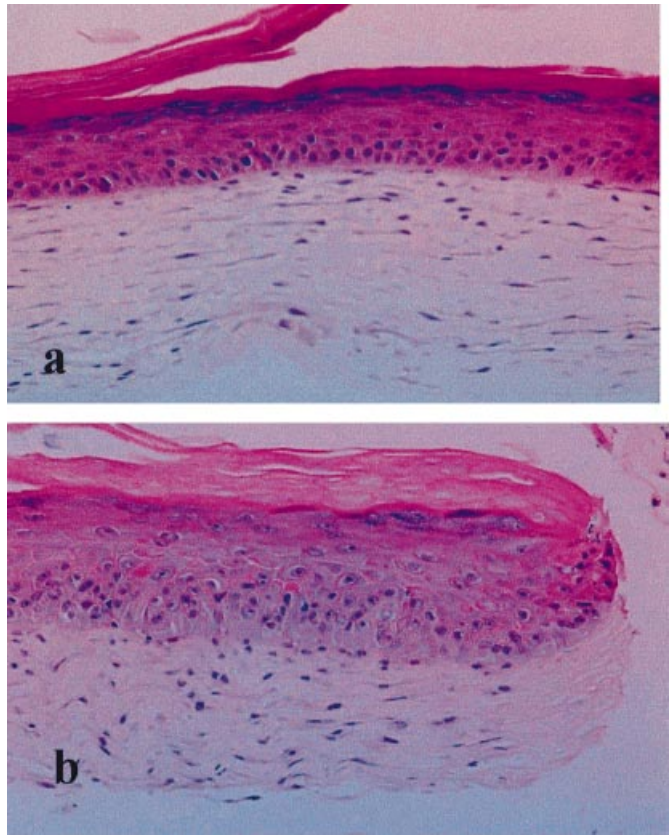


**Figure 3. Histologic appearance of the HBSS.** (*a*) Before injury by meshing; (*b*) 24 h after injury by meshing at a ratio of 1.5–1. 20×.

## RESULTS

***In vitro* reepithelialization of HBSS** The ability over time of the HBSS keratinocytes to migrate and close the wound in vitro was determined by placing the entire bilayered construct over a separate dermal equivalent (lower portion of HBSS). This was done to more closely mimic in vivo wounding. The initial wounds were approximately 4 mm in length. As shown in **Fig 2**, by 12 h an epithelial tongue was seen at the wound margin as keratinocytes began to migrate from the edges. Keratinocyte migration continued over the next 2 d. By day 2, the wound was completely reepithelialized with a multilayer of keratinocytes. By day 4 the wound was completely covered with a well-differentiated epidermis including a stratum corneum. In other experiments, the HBSS response to injury was determined by keeping the construct over its nutrient agar. There were histologic differences between wounded and nonwounded HBSS in these experiments.

The nonwounded HBSS has a well-defined basal layer and a compact stratum corneum (**Fig 3**). By 24 h after wounding, a very noticeable change in the epidermal architecture was appreciated. As shown in **Fig 3**, there was disruption of the granular layer, and the epidermal cells acquired a more squamous-cell-like morphology, with a less-defined basal layer. These morphologic changes observed by histology point to an epidermis that has shifted to a migratory state. This question was studied further by immunohistochemistry and by staining for Ki67, a marker of proliferation (Andreadis *et al*, 2001). As shown in **Fig 4**, nonwounded HBSS had a high and regularly spaced number of proliferating basal cell keratinocytes. Twenty-four hours after wounding of the construct, however, one could see focally diminished staining for Ki67 (**Fig 4**). In particular, there was markedly less staining at the advancing epidermal tongue and grouping of proliferating keratinocytes away from the edges. These findings were present in all wounded specimens, either meshed or perforated, and suggest that wounding of the construct is associated with a dramatic shift of the basal keratinocytes from a proliferative to a migratory state. To study this process further, we determined the entry of cells into the S phase of the cell cycle. As shown in **Fig 5**, simply lifting the bioengineered skin construct from its nutrient transwell was associated with an increase in the percentage of cells entering the S phase. In agreement with the immunohistochemical studies with Ki67, however, wounding led to a decrease in the percentage of cells entering S phase. This result was seen after injury by either meshing or fenestration, and was observed in eight out of eight experiments ($p < 0.01$). The dermal component of HBSS also underwent histologic and immunohistochemical changes indicative of increased proliferation and synthetic activity. In particular, the dermal component was approximately 20% greater in size, with a greater number of fibroblasts (data not shown).

**Cytokine and growth factor expression after injury** The histologic and immunohistochemical changes just described were accompanied by substantial alterations in the pattern of pro-inflammatory cytokines and growth factors, as measured by RT-PCR. These results are shown in **Figs 6–9**. **Figures 6** and **7** illustrate representative blots, whereas **Figs 8** and **9** represent the summary of determinations of at least three separate experiments for each cytokine and growth factor level. As can be seen from **Figs 8** and **9**, there is a staged progression of cytokine and growth factor production. In general, an increase in the levels of pro-inflammatory cytokines (IL-1α, IL-1β, IL-6, IL-8, IL-11, and TNF-α) is observed quickly, in the first 12 h. The time by which maximal levels of these cytokines are observed was different, however. For example, IL-1α and TNF-α levels showed maximal production by 24 h, whereas IL-1β and IL-11 were maximal by 12 and 72 h, respectively. In contrast, the levels of growth factors increased at later time points. For example, as seen in **Figs 8** and **9**, insulin-like growth factor 2 (IGF-2) and TGF-β1 levels did not increase until 48 h after injury to the construct. In some cases, such as with TGF-α and TGF-β3, no significant increase was observed throughout the observation period. In the case of platelet-derived growth factor B (PDGF-B), peak production activity was seen after 72 h.

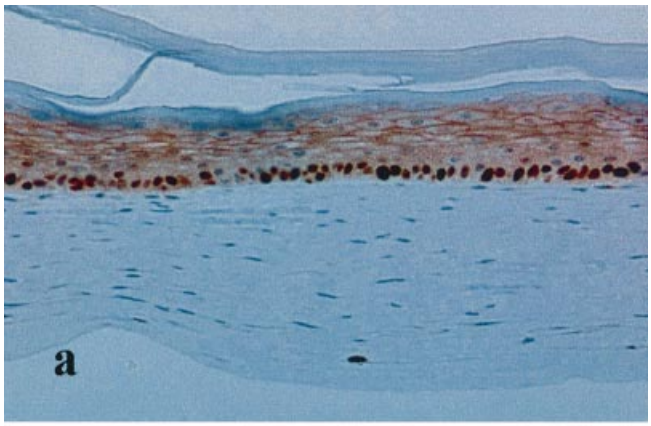


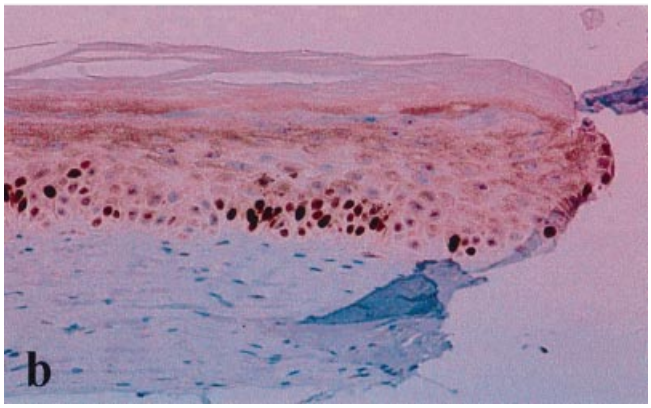


**Figure 4. Immunohistochemical staining for Ki67 of the HBSS.** (*a*) Before injury by meshing; (*b*) 24 h after injury by meshing at a ratio of 1.5–1. 20×.

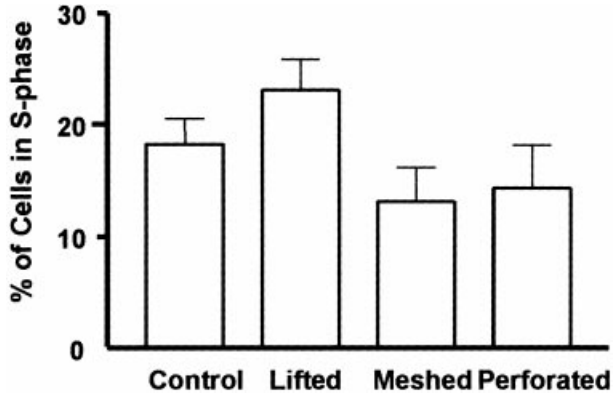


**Figure 5. Results of flow cytometry indicating entry into S phase of the keratinocyte component of the HBSS after injury by meshing or by fenestration (perforation) with a scalpel.** Results represent the mean ± SD from eight experiments.

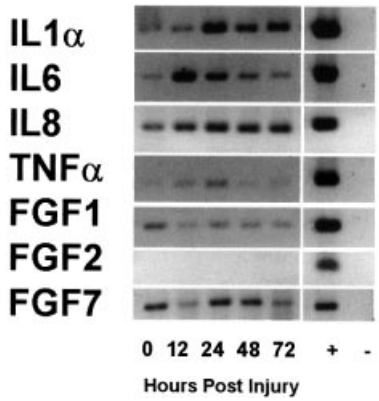


**Figure 6. Levels of pro-inflammatory cytokines, as measured by RT-PCR, in the HBSS at various intervals after meshing injury.** The figure shows a representative blot.

The staged alteration in cytokine and growth factor expression observed by PCR was also demonstrable at the protein level for selected cytokines we measured. These measurements were performed by ELISA and immunohistochemistry. As early as 4 h postinjury, significant levels of IL-1α protein levels were detected in the culture supernatant (**Fig 10**), with peak concentrations observed by 24 h. An increase in IL-6 mRNA accumulation had been observed 4 h postinjury by RT-PCR. As shown in **Fig 11**, IL-6 protein was detected in the culture supernatant 8 h later and continued to increase over the next 48 h. PDGF was detected in cell lysates at 24 h postinjury with continued protein accumulation over the next 3 d (not shown). It should be noted that the extent of injury to the HBSS is also important. Thus, using RT-PCR 24 h after injury to HBSS, we found that, compared to scalpel injury, meshing injury increases the levels of cytokines (data not shown). This finding was most notable for IL-1α (318%), IL-11 (250%), IL-6 (150%), and IL-8 (135%).

Dynamic changes in the production of cytokines and growth factors by HBSS after injury were in large part due to the epidermal component. To determine this, we measured mRNA levels by RT-PCR in studies where the dermal equivalent of HBSS (prepared without the keratinocyte component) was injured by mincing with a scalpel. In these experiments (actual results now shown), if a band had a relative intensity of < 0.05 after correcting for GAPDH, it was considered negative. The 0.05 level was determined by a serial dilution of a GAPDH PCR product on an ethidium bromide stained agarose gel, and a measure was taken of the lane next to the last visible band. Baseline levels, before injury, are represented by day 7 postcast of the dermal equivalent. We found a 3-fold increase in the levels of IL-1 and IGF-2 at days 14 and 21 postcasting ($p < 0.05$). Conversely, the levels of most cytokines and growth factors were already maximal in the dermal equivalent at baseline. This was true of IL-6, IL-8, TGF-β1, TGF-β3, IGF-1, connective tissue growth factor, TGF-α, fibroblast growth factor 7 (FGF-7), and vascular endothelial growth factor (VEGF).

To obtain a visual representation of the changes in expression of pro-inflammatory cytokines and growth factors demonstrated by RT-PCR and by measurements of protein levels, we performed immunohistochemistry using antibodies to TNF-α and TGF-β1. **Figure 12** shows how TNF-α is expressed by basal cells early after injury, with maximum expression between 12 and 24 h. Conversely, as shown in **Fig 13**, TGF-β1 was increasingly expressed much later after injury, as observed by 72 h. By this time point, there was intense expression of TGF-β1 not only in the epidermis but also in dermal fibroblasts, with evidence of dermal thickening and increased fibroblast number. Interestingly, the distribution of these cytokines and their intensities did not differ at the center of the bioengineered skin construct compared to its meshed edge, suggesting that perhaps the signals of injury are propagated over substantial distances.

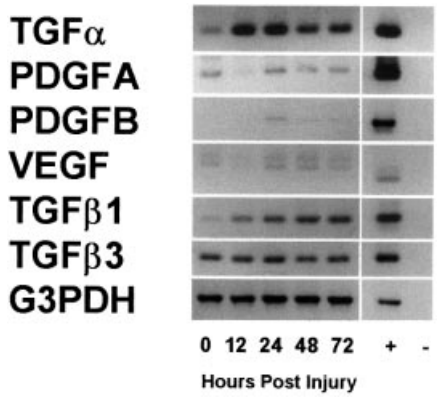


**Figure 7. Levels of growth factors, as measured by RT-PCR, in the HBSS at various intervals after meshing injury.** The figure shows a representative blot.

## DISCUSSION

We report that bioengineered skin, as shown here with a living bilayered skin construct, is capable of defined cellular and molecular responses after wounding. These responses appear to mimic the *in vivo* repair process (Singer and Clark, 1999; Freedberg *et al*, 2001) and can provide fundamental insights into wound healing. Thus, we have demonstrated that an HBSS is able to reepithelialize itself and to undergo a staged response to wounding in terms of the production of pro-inflammatory cytokines (early) and growth factors (late). The process of reepithelialization appears to be associated with a marked shift of keratinocytes from proliferation to migration. Together, these findings indicate the potential of this *in vitro* model to enhance our understanding of the healing process

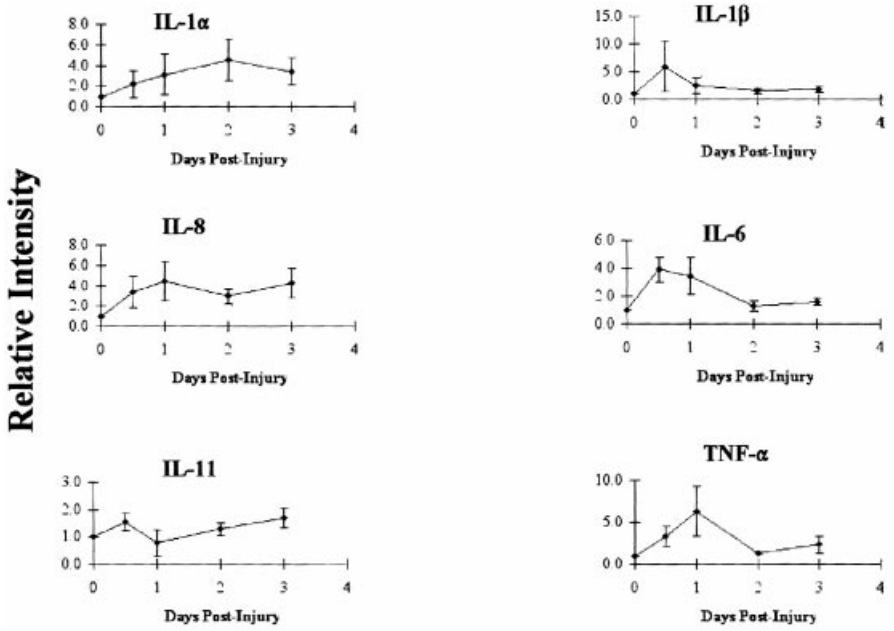


**Figure 8. Levels of cytokines (mean ± SD), as measured by RT-PCR, in the HBSS at various times after meshing injury.** For these experiments, the stained gels were photographed and subsequently digitally captured using a CCD camera. Intensities of band products were quantified using image software (ImagePro, CA). Each of the cytokines was corrected for varying amounts of RNA by normalizing to GAPDH. Each experiment was repeated at least three times.

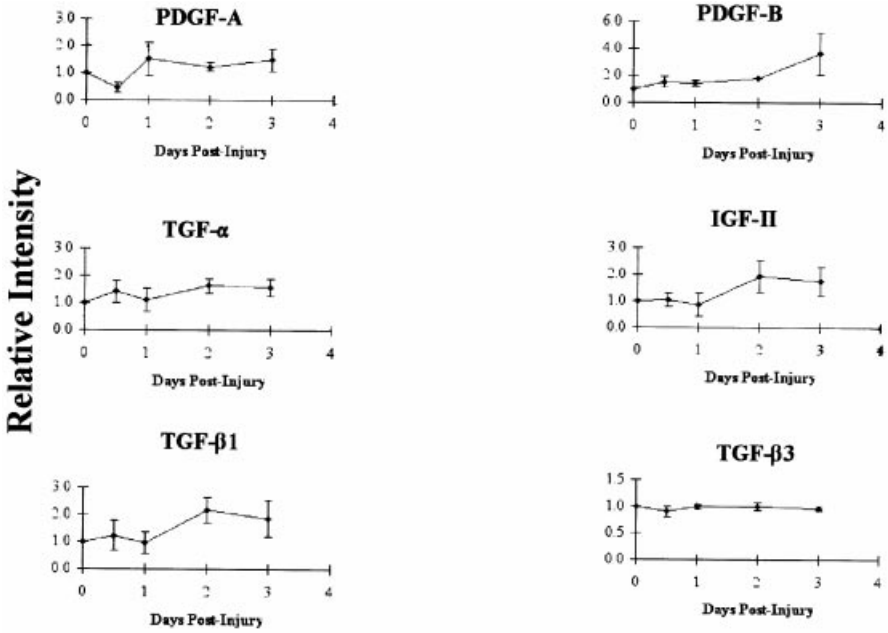


**Figure 9. Levels of growth factors (mean ± SD), as measured by RT-PCR, in the HBSS at various times after meshing injury.** For these experiments, the stained gels were photographed and subsequently digitally captured using a CCD camera. Intensities of band products were quantified using image software (ImagePro, CA). Each of the cytokines was corrected for varying amounts of RNA by normalizing to GAPDH. Each experiment was repeated at least three times.

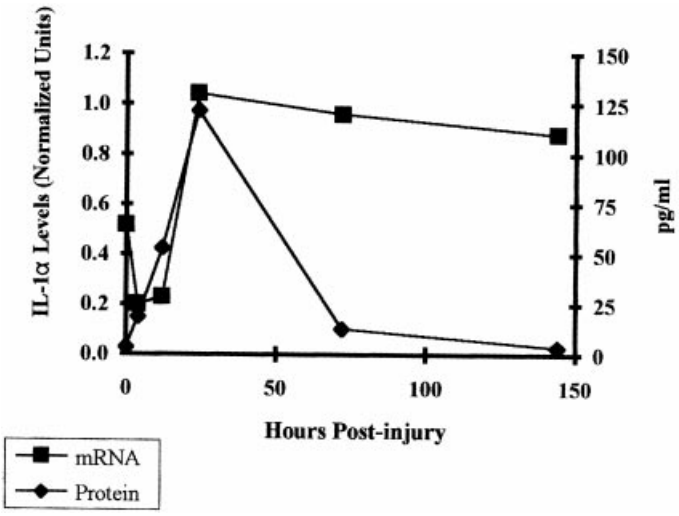


**Figure 10. Protein levels of IL-1α, as measured by ELISA, and mRNA levels in the HBSS after meshing injury.** Each point represents the mean of triplicate determinations.

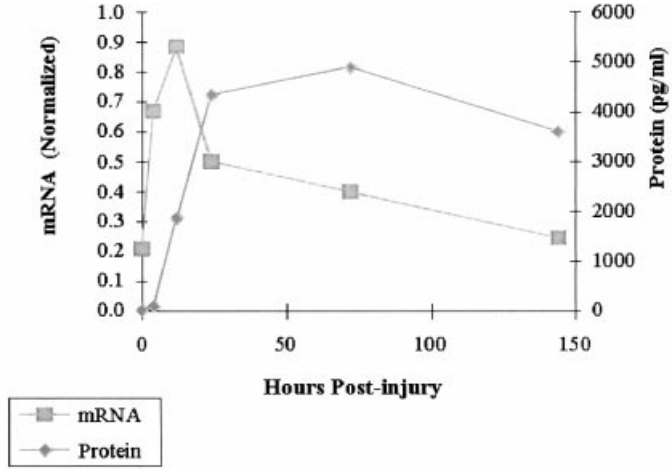


**Figure 11. Protein levels of IL-6, as measured by ELISA, and mRNA levels in the HBSS after meshing injury.** Each point represents the mean of triplicate determinations.

and provide critical insights into the possible mechanisms of action of bioengineered skin. Admittedly, further studies will be needed to precisely link the changes we have observed in the bioengineered construct studied in this report with human skin treated the same way.

The finding that HBSS is able to reepithelialize itself after meshing is in agreement with a previous more limited observation (Garlick and Taichman, 1994). We chose here to place the meshed HBSS over a bed composed of the isolated dermal component of the construct. In our opinion, this situation mimics more closely the *in vivo* setting, where bioengineered skin is placed over a dermal bed. It should be noted, however, that migration and resurfacing are also observed after the construct is placed over tissue culture plastic. Indeed, it appears that the time required for reepithelialization is actually faster over plastic, with resurfacing observed by 24 h (Milstone *et al*, 2000). It may very well be that plastic represents continued and greater injury to the construct or that the fibroblast-rich dermal matrix may actually slow down epithelial resurfacing. This discrepancy is of more than passing interest, because it provides us with a theoretical view that the construct is capable of even faster migratory activity. Studying the possible mechanisms involved may perhaps enhance the clinical effectiveness of these constructs. Of great interest is the shift we observed from a high proliferative to a migratory state of HBSS after wounding. The effect was quite marked, as shown by histology, immunohistochemistry, and flow cytometry, and suggests that, when wounded, the cellular components of human skin, particularly keratinocytes, may also shift from proliferation to migration. This relationship between migration and proliferation, which has been previously described (Fransson and Hammar, 1992; Sarret *et al*, 1992; Woodley *et al*, 1993), makes both theoretical and practical sense, for it is difficult if not impossible for cells to migrate and proliferate at the same time. There could be some useful manipulations of this system, which we did not try in these studies. For example, it is

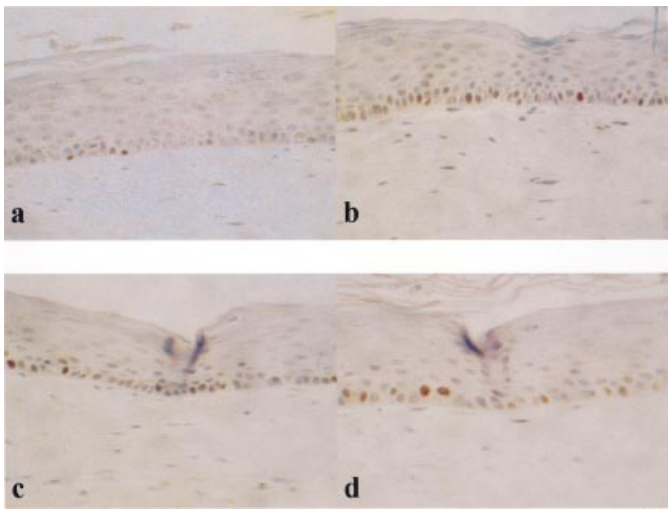


**Figure 12. Immunohistochemical staining for TNF-α in the HBSS at various times after injury by meshing.** (*a*) Baseline; (*b*) 12 h; (*c*) 24 h; (*d*) 48 h. 20×.

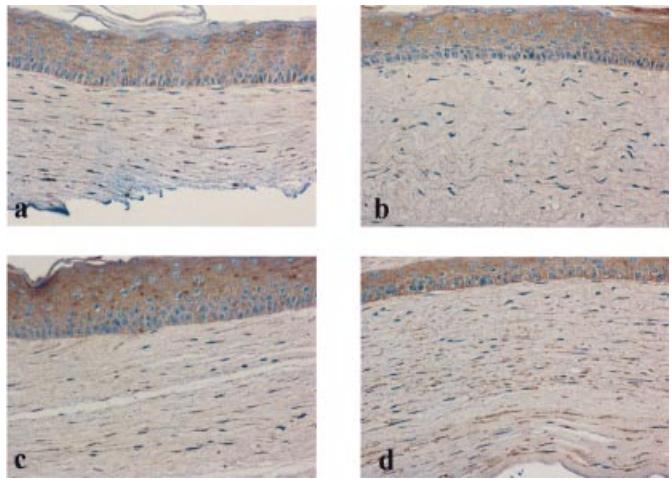


**Figure 13. Immunohistochemical staining for TGF-β1 in the HBSS at various times after injury by meshing.** (*a*) 12 h; (*b*) 24 h; (*c*) 48 h; (*d*) 72 h.

theoretically possible that by priming the skin with an antiproliferative agent we might be able to enhance the "migratory shift". Regardless, this finding provides useful insights into the healing process and, with additional studies comparing these findings with those observed with human skin, could represent proof of principle of the value of bioengineered skin as a model for wounding and for generating additional hypotheses. Our results are consistent with previous findings demonstrating delayed proliferation following an initial migratory phase (Winter, 1962). More indirectly, others have shown individual genetically marked cells within the wound bed, indicating that individual cells had migrated from the wound edges without having undergone replication (Garlick and Taichman, 1994). Another useful question is whether bioengineered skin could cause a "migratory shift" within wounds. This idea is supported by the clinical observations that skin substitutes, including keratinocyte sheets, cause an "edge effect", with rather dramatic migration of keratinocytes from the wound's edges (Falanga, 2000*b*).

The first phase of wound healing is characterized by a number of overlapping events, including the production of pro-inflammatory cytokines. This pro-inflammatory stage occurs within the first 24 h after injury. IL-1α and TNF-α represent the primary cytokines for pro-inflammatory responses. IL-1α upregulates the production of IL-6, IL-8, and TGF-α (Ansel *et al*, 1990). In addition, keratinocytes maintain substantial amounts of IL-1α in intracellular stores. These stores are released when a biologic or mechanical insult occurs in the skin. In this study we detected increased levels of IL-1α in the culture supernatant 4–12 h postinjury, pointing to the rapid release of this cytokine from its intracellular stores. A direct effect of IL-1 release is the upregulation of IL-6 production. By 12 h, we observed an increase in IL-6 mRNA levels. IL-6 has been associated with the release of colony stimulating factors (CSFs) by keratinocytes and with an increase of acute phase proteins in serum (Imokawa *et al*, 1996). Although not shown, we found increased CSF production in HBSS after injury. There is a cascade of these pro-inflammatory cytokines, which has been found *in vivo* and which was clearly reproduced in these studies. Another example is IL-8, a chemokine with angiogenic properties (Koch *et al*, 1992). Similarly to IL-6, IL-8 is upregulated by the release of IL-1. Consistent with this upregulation, we found its mRNA levels to be increased by 12 h.

The second phase of wound healing is associated with growth-oriented cytokines and factors, capable of initiating extracellular matrix deposition and cellular proliferation. Generally, this stage begins early (4–12 h) from the time of injury and can last longer than the inflammatory stage (> 6 d). IGF-2, PDGF-A, PDGF-B, TGF-βs, and VEGF are all upregulated during the growth phase of cutaneous repair, and this is the reason why we determined their levels in this study. We found that the levels of these cytokines and growth factors were upregulated in wounded HBSS after 24 h, a timing quite consistent with what has been observed *in vivo*. The TGF-βs have multiple functions throughout wound healing, including playing a critical role in the deposition of extracellular matrix proteins and preventing hyperproliferation of keratinocytes after wound closure (Roberts *et al*, 1986). In this study, TGF-β1 mRNA was upregulated by 24 h and TGF-β3 was constitutively expressed. Taken together, our findings with HBSS closely follow the pattern reported after *in vivo* injury to the skin.

In summary, using a prototypic bilayered living skin construct, we report that bioengineered skin acts as a living tissue, capable of appropriately responding to wounding injury. We expect that other types of living skin substitutes will behave similarly, particularly if their structure allows for dermal–epidermal interactions. Our results also suggest that the accelerated healing observed with the therapeutic use of these constructs may be related to their ability to deliver a cascade of cytokines and growth factors. In many ways, as indicated by our results, bioengineered skin behaves like an acute wound. It is interesting to consider that, when these constructs are used therapeutically in difficult to heal wounds, they may be acting as an "acute wound" placed in a chronic wound, and thus are able to re-condition and reset the healing environment.

*This work was supported by grants to Dr. Falanga from the National Institutes of Health (AR42936 and AR46557) and the Wound Biotechnology Foundation.*

## REFERENCES

Andreadis ST, Hamoen KE, Yarmush ML, Morgan JR: Keratinocyte growth factor induces hyperproliferation and delays differentiation in a skin equivalent model system. *FASEB J* 5:898–906, 2001

Ansel J, Perry P, Brown J, *et al*: Cytokine modulation of keratinocyte cytokines. *J Invest Dermatol* 94:101S–107S, 1990

Brain A, Purkis P, Coates P, *et al:* Survival of cultured allogeneic keratinocytes transplanted to deep dermal bed assessed with probe for Y chromosome. *Br Med J* 298:917–919, 1989

Brem H, Balledux J, Sukkarieh T, Carson P, Falanga V: Healing of venous ulcers of long duration with a bilayered living skin substitute: results from a general surgery and dermatology department. *Dermatol Surg* 27:915–919, 2001

Falanga V: Classifications for wound bed preparation and stimulation fo chronic wounds. *Wound Rep Regen* 8:347–352, 2000*a*

Falanga V: Tissue engineering in wound repair. *Adv Skin Wound Care* 13:15–29, 2000*b*

Falanga V, Margolis D, Alvarez O, et al: Healing of venous ulcers and lack of clinical rejection with an allogeneic cultured human skin equivalent. *Arch Dermatol* 134:293–300, 1998

Fransson J, Hammar H: Epidermal growth in the skin equivalent. *Arch Dermatol Res* 284:343–348, 1992

Freedberg IM, Tomic-Canic M, Komine M, Blumenberg M: Keratins and the keratinocyte activation cycle. *J Invest Dermatol* 116:633–640, 2001

Garlick JA, Taichman LB: Effect of TGF-beta 1 on re-epithelialization of human keratinocytes *in vitro*: an organotypic model. *J Invest Dermatol* 103:554–559, 1994

Imokawa G, Yada Y, Kimura M, Morisaki N: Granulocyte/macrophage colony-stimulating factor is an intrinsic keratinocyte-derived growth factor for human melanocytes in UVA-induced melanosis. *Biochem J* 313:625–631, 1996

Koch A, Polverini P, Kunkel S, *et al:* Interleukin 8 as a macrophage derived mediator of angiogenesis. *Science* 258:1798–1801, 1992

Milstone LM, Asgari MM, Schwartz PM, Hardin-Young J: Growth factor expression, healing, and structural characteristics of Graftskin (Apligraf). *Wounds* 12:12A–19A, 2000

Phillips TJ: New skin for old; developments in biological skin substitutes. *Arch Dermatol* 134:344–349, 1998

Phillips TJ, Manzoor J, Rojas A, et al: The longevity of a bilayered skin substitute after application to venous ulcers. *Arch Dermatol*, in press

Roberts AB, Sporn MB, Assoian RK, *et al*: Transforming growth factor type beta. Rapid induction of fibrosis and angiogenesis *in vivo* and stimulation of collagen formation *in vitro*. *Proc Natl Acad Sci* 83:4167–4171, 1986

Sarret Y, Woodley DT, Grigsby K, Wynn K, O'Keefe EJ: Human keratinocytes locomotion: the effect of selected cytokines. *J Invest Dermatol* 98:12–16, 1992

Singer AJ, Clark RAF: Cutaneous wound healing. *N Engl J Med* 341:738–746, 1999

Veves A, Falanga V, Armstrong DG, Sabolinski ML: Graftskin, a human skin equivalent, is effective in the treatment of non-infected neuropathic diabetic foot ulcers: a prospective randomized clinical trial. *Diabetes Care*, 2001

Wilkins LM, Watson SR, Prosky SJ, Meunier SF, Parenteau NL: Development of bilayered living skin construct for clinical application. 24:290–295, *Biotech Bioengineering* 43:747–756, 1994

Winter GD: Formation of scab and the rate of epithelialization of superficial wounds in the skin of the young domestic pig. *Nature* 193:293–294, 1962

Woodley DT, Chen JD, Kim JP, Sarret Y, Iwasaki T, Kim YH, O'Keefe EJ: Re-epithelialization. Human keratinocytes locomotion. *Dermatol Clin* 11:641–646, 1993